

shifting of the IT band seen for the alternating stack and clay-intercalated cations is attributable to an increase in the zero-point energy difference between the two vibronic states of the mixed-valence cation. This results from intermolecular interactions enhanced by pressure.

The red shift of the IT band that dominates the high-pressure response is attributable to an intramolecular effect, namely a reduction of the vibronic coupling in the mixed-valence cation. Thus, under high pressures, the difference between Fe<sup>II</sup>-C and Fe<sup>III</sup>-C bond lengths is reduced, which reduces the vibronic coupling.

The major conclusion from this study is that the physical properties of these mixed-valence biferrocenium cations depend strongly on the solid-state environments. It would be quite in-

teresting to monitor the rate of electron transfer of such a mixed-valence complex as the applied pressure is increased. This could be done indirectly by spectroscopic means such as <sup>57</sup>Fe Mössbauer spectroscopy.

**Acknowledgment.** This work was supported in part by the Materials Science Division, Department of Energy, under Contract DE-ACO2-76ER01198 and in part by NIH Grant HL13652.

**Registry No.** 1, 39470-17-2; 2, 70282-49-4; 3, 56030-43-4; 4, 103752-22-3; 5, 88005-31-6; 6, 88005-33-8; 7, 78713-00-5; 8, 96898-15-6.

**Supplementary Material Available:** Tables I-VII of changes of  $E_{\max}$  vs pressure data for the IT bands (7 pages). Ordering information is given on any current masthead page.

## Stereochemistry of Crown Ethers and Their Complexes in the Solid State. <sup>13</sup>C CPMAS NMR and X-ray Crystallographic Studies of Configurationally Isomeric Dicyclohexano-14-crown-4 Ethers, Dibenzo-14-crown-4 Ether, and Some Lithium Thiocyanate Salts

G. W. Buchanan,\*† R. A. Kirby,† and J. P. Charland‡

Contribution from the Ottawa—Carleton Chemistry Institute, Department of Chemistry, Carleton University, Ottawa, Canada K1S 5B6, and Division of Chemistry, National Research Council of Canada, Ottawa, Canada K1A 0R9. Received July 27, 1987

**Abstract:** For the cis-anti-cis and cis-syn-cis isomers of dicyclohexano-14-crown-4 and one LiNCS complex, X-ray crystallographic data are presented along with solid-phase <sup>13</sup>C NMR spectra. Clear evidence for inversion of one of the cyclohexane rings of the cis-syn-cis isomer in order to form the LiNCS complex is presented. Other structural features of these systems are discussed in detail as well as the geometrical dependence of <sup>13</sup>C chemical shifts in solids. For the dibenzo-14-crown-4 complex with LiNCS the solid-phase <sup>13</sup>C NMR spectral results are discussed in light of the known X-ray structure.

In crown ether chemistry, the 14-crown-4 system is of interest because of its nearly ideal cavity dimensions for complexation of the lithium ion. For the parent 14-crown-4 ether molecule, the X-ray crystal structure, determined at -150 °C, has been published.<sup>1</sup> For dibenzo-14-crown-4, the structure of its LiNCS complex has also been determined via X-ray techniques.<sup>2</sup> By contrast, little is known regarding the solid-state structure of dicyclohexano derivatives of the 14-crown-4 system.

Recently<sup>3,4</sup> we have found that solid-phase <sup>13</sup>C NMR is a powerful method for the determination of asymmetric units in a series of dicyclohexano-18-crown-6 ethers. Interpretation of such spectra, however, can be complicated by crystal packing phenomena or the existence of different crystal forms in the solid.<sup>5</sup> Hence inclusion of available X-ray data in any discussion of <sup>13</sup>C CPMAS spectra is required.

With the solid-phase <sup>13</sup>C chemical shifts in hand along with the corresponding X-ray data, the opportunity exists for detailed analysis of stereochemical contributions to carbon shieldings.

### Results and Discussion

The structural formulae and numbering schemes for the molecules studied herein are depicted in Figure 1. The numbering schemes employed are chosen to be consistent with the X-ray data output rather than with IUPAC convention. Bond lengths and angles for cis-anti-cis-dicyclohexano-14-crown-4 (**1**), the corre-

sponding cis-syn-cis isomer **2**, and the LiNCS complex of **2** are listed in Table I. Torsion angles involving ring skeletal atoms for these three systems are provided in Table II along with data for 14-crown-4 itself. Figure 2 shows stereoviews of **1**, **2**, and the LiNCS complex of **2** while Figure 3 contains the <sup>13</sup>C CPMAS spectra of these systems. In Figure 4 are presented the <sup>13</sup>C CPMAS spectra of dibenzo-14-crown-4 and its LiNCS complex. Table III contains the <sup>13</sup>C solid-phase chemical shifts for the five systems examined herein.

(i) *cis-anti-cis*-Dicyclohexano-14-crown-4 (**1**). In solution,<sup>6</sup> under low-temperature conditions where ring inversion is slow on the <sup>13</sup>C NMR time scale, this molecule has been shown to exist as a mixture of two conformations in the ratio of ca. 2:1. The <sup>13</sup>C CPMAS spectrum (Figure 3) of solid **1**, however, suggests the presence of only one conformation in the crystal, since only nine resonances are observed.

Figure 2 shows that **1** has a local center of symmetry from the molecular standpoint. Averages over pairs of presumed symmetry related non-hydrogen positions of **1** were calculated and yielded

(1) Groth, P. *Acta Chem. Scand.* **1978**, *32*, 91.

(2) Shoham, G.; Lipscomb, W. N.; Olsner, U. *J. Chem. Soc., Chem. Commun.* **1983**, 208.

(3) Buchanan, G. W.; Ripmeester, J. A.; Bovenkamp, J. W.; Rodrigue, A. *Tetrahedron Lett.* **1986**, *27*, 2239.

(4) Buchanan, G. W.; Khan, M. Z.; Ripmeester, J. A.; Bovenkamp, J. W.; Rodrigue, A. *Can. J. Chem.* **1987**, *65*, 2564.

(5) Belton, P. S.; Tanner, S. F.; Wright, K. M.; Payne, M. P.; Truter, M. R.; Wingfield, J. N. *J. Chem. Soc., Perkin Trans. 11* **1985**, 1307.

(6) Buchanan, G. W.; Kirby, R. A. *Tetrahedron Lett.* **1987**, *28*, 1507.

\* Author to whom correspondence should be addressed.

† Carleton University.

‡ National Research Council of Canada.

Table I. Bond Lengths (Å) and Bond Angles (deg) for 1, 2, and 2·LiNCS

1							
O(1)-C(1)	1.405 (5)	O(2')-C(9)	1.404 (7)	C(4)-C(5)	1.496 (12)	C(2')-C(3')	1.538 (8)
O(1)-C(7)	1.436 (7)	O(2')-C(2')	1.436 (10)	C(5)-C(6)	1.535 (10)	C(3')-C(4')	1.494 (10)
O(2)-C(2)	1.412 (10)	C(1)-C(2)	1.504 (8)	C(7)-C(8)	1.530 (7)	C(4')-C(5')	1.536 (11)
O(2)-C(9')	1.445 (7)	C(1)-C(6)	1.556 (9)	C(8)-C(9)	1.518 (10)	C(5')-C(6')	1.494 (10)
O(1')-C(1')	1.433 (6)	C(2)-C(3)	1.506 (8)	C(1')-C(2')	1.510 (8)	C(7')-C(8')	1.511 (8)
O(1')-C(7')	1.424 (6)	C(3)-C(4)	1.552 (11)	C(1')-C(6')	1.529 (10)	C(8')-C(9')	1.517 (10)
C(1)-O(1)-C(7)	111.9 (4)	O(2)-C(2)-C(3)	106.7 (5)	O(2')-C(9)-C(8)	106.7 (5)	C(2')-C(3')-C(4')	111.2 (6)
C(2)-O(2)-C(9')	114.6 (5)	C(1)-C(2)-C(3)	112.6 (5)	O(1')-C(1')-C(2')	108.4 (4)	C(3')-C(4')-C(5')	112.3 (6)
C(1')-O(1')-C(7')	113.5 (4)	C(2)-C(3)-C(4)	111.7 (6)	O(1')-C(1')-C(6')	110.1 (5)	C(4')-C(5')-C(6')	111.7 (7)
C(9)-O(2')-C(2')	114.5 (4)	C(3)-C(4)-C(5)	111.1 (6)	C(2')-C(1')-C(6')	110.2 (5)	C(1')-C(6')-C(5')	112.2 (6)
O(1)-C(1)-C(2)	107.3 (4)	C(4)-C(5)-C(6)	110.9 (6)	O(2')-C(2')-C(1')	113.7 (5)	O(1')-C(7')-C(8')	108.3 (4)
O(1)-C(1)-C(6)	111.1 (4)	C(1)-C(6)-C(5)	110.8 (5)	O(2')-C(2')-C(3')	107.9 (5)	C(7')-C(8')-C(9')	113.8 (5)
C(2)-C(1)-C(6)	109.7 (5)	O(1)-C(7)-C(8)	108.3 (4)	C(1')-C(2')-C(3')	112.2 (5)	O(2)-C(9')-C(8')	106.8 (5)
O(2)-C(2)-C(1)	114.3 (4)	C(7)-C(8)-C(9)	113.6 (5)				
2							
O(1)-C(1)	1.4275 (22)	O(2')-C(9)	1.4239 (23)	C(4)-C(5)	1.516 (4)	C(2')-C(3')	1.517 (3)
O(1)-C(7)	1.4133 (23)	O(2')-C(2')	1.4285 (22)	C(5)-C(6)	1.527 (3)	C(3')-C(4')	1.520 (3)
O(2)-C(2)	1.4272 (23)	C(1)-C(2)	1.523 (3)	C(7)-C(8)	1.508 (3)	C(4')-C(5')	1.513 (4)
O(2)-C(9')	1.4239 (23)	C(1)-C(6)	1.512 (3)	C(8)-C(9)	1.503 (3)	C(5')-C(6')	1.525 (3)
O(1')-C(1')	1.4229 (22)	C(2)-C(3)	1.519 (3)	C(1')-C(2')	1.522 (3)	C(7')-C(8')	1.505 (3)
O(1')-C(7')	1.4241 (23)	C(3)-C(4)	1.507 (4)	C(1')-C(6')	1.517 (3)	C(8')-C(9')	1.499 (3)
C(1)-O(1)-C(7)	116.10 (14)	O(2)-C(2)-C(3)	106.67 (17)	O(2')-C(9)-C(8)	108.65 (17)	C(2')-C(3')-C(4')	111.24 (16)
C(2)-O(2)-C(9')	114.29 (15)	C(1)-C(2)-C(3)	110.26 (18)	O(1')-C(1')-C(2')	107.29 (15)	C(3')-C(4')-C(5')	111.56 (20)
C(1')-O(1')-C(7')	116.51 (15)	C(2)-C(3)-C(4)	111.79 (20)	O(1')-C(1')-C(6')	114.35 (15)	C(4')-C(5')-C(6')	112.26 (19)
C(9)-O(2')-C(2')	114.56 (14)	C(3)-C(4)-C(5)	111.42 (22)	C(2')-C(1')-C(6')	110.46 (17)	C(1')-C(6')-C(5')	110.79 (17)
O(1)-C(1)-C(2)	106.83 (15)	C(4)-C(5)-C(6)	111.28 (21)	O(2')-C(2')-C(1')	111.31 (14)	O(1')-C(7')-C(8')	107.75 (18)
O(1)-C(1)-C(6)	114.64 (16)	C(1)-C(6)-C(5)	110.99 (20)	O(2')-C(2')-C(3')	107.32 (16)	C(7')-C(8')-C(9')	112.94 (18)
C(2)-C(1)-C(6)	111.05 (18)	O(1)-C(7)-C(8)	108.55 (17)	C(1')-C(2')-C(3')	110.01 (17)	O(2)-C(9')-C(8')	108.64 (17)
O(2)-C(2)-C(1)	111.23 (15)	C(7)-C(8)-C(9)	114.39 (18)				
2·LiNCS							
S-C(11)	1.625 (6)	O(2)-Li	2.074 (6)	C(2)-C(3)	1.533 (5)	C(8)-C(7)a	1.513 (5)
O(1)-C(1)	1.449 (4)	N-C(11)	1.145 (8)	C(3)-C(4)	1.527 (8)	C(9)-C(10)	1.526 (5)
O(1)-C(7)	1.417 (4)	N-Li	2.029 (10)	C(4)-C(5)	1.513 (8)	C(10)-C(9)a	1.526 (5)
O(1)-Li	1.958 (6)	C(1)-C(2)	1.508 (5)	C(5)-C(6)	1.535 (6)	Li-O(1)a	1.958 (6)
O(2)-C(2)	1.448 (4)	C(1)-C(6)	1.521 (6)	C(7)-C(8)	1.513 (5)	Li-O(2)a	2.074 (6)
O(2)-C(9)	1.428 (5)						
C(1)-O(1)-C(7)	115.6 (3)	O(1)-C(1)-C(6)	111.3 (3)	C(1)-C(6)-C(5)	109.7 (4)	O(1)-Li-O(2)a	148.8 (5)
C(1)-O(1)-Li	113.98 (25)	C(2)-C(1)-C(6)	112.2 (3)	O(1)-C(7)-C(8)	108.7 (3)	O(1)-Li-N	108.6 (3)
C(7)-O(1)-Li	128.5 (3)	O(2)-C(2)-C(1)	105.7 (3)	C(7)-C(8)-C(7)a	115.2 (4)	O(1)a-Li-O(2)	148.8 (5)
C(2)-O(2)-C(9)	114.7 (3)	O(2)-C(2)-C(3)	113.5 (3)	O(2)-C(9)-C(10)	108.6 (4)	O(1)a-Li-O(2)a	81.51 (14)
C(2)-O(2)-Li	103.21 (22)	C(1)-C(2)-C(3)	110.1 (3)	C(9)-C(10)-C(9)a	116.1 (4)	O(1)a-Li-N	108.6 (3)
C(9)-O(2)-Li	113.4 (3)	C(2)-C(3)-C(4)	110.8 (4)	S-C(11)-N	179.0 (5)	O(2)-Li-O(2)a	88.9 (3)
C(11)-N-Li	147.7 (5)	C(3)-C(4)-C(5)	110.6 (3)	O(1)-Li-O(1)a	91.5 (4)	O(2)-Li-N	102.4 (3)
O(1)-C(1)-C(2)	105.8 (3)	C(4)-C(5)-C(6)	110.9 (4)	O(1)-Li-O(2)	81.51 (14)	O(2)a-Li-N	102.4 (3)

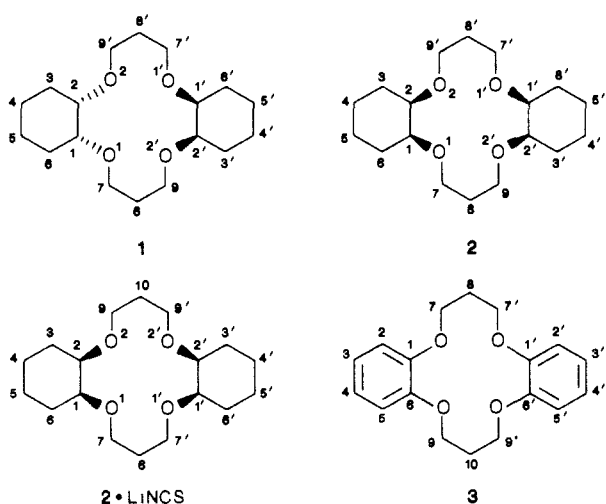


Figure 1. Structural formulas and numbering schemes.

the location of the molecular center: (.751 (2), .314 (1), .912 (1)). This additional evidence clearly supports the correctness of the space group, as the coordinates of this center are *not* those which the molecule would occupy on a crystallographic center of symmetry in *Pbcm*. More importantly, the standard deviations in the

coordinates of the molecular center of symmetry are of the same order of magnitude as the standard deviations in the atomic coordinates. Hence, the molecular center of symmetry in **1** can be regarded as being a "true" local (or molecular) center and not a crystallographic center.

With respect to the  $^{13}\text{C}$  chemical shifts in solid **1**, a number of interesting trends exist. The lowest field absorption at 78.02 ppm arises from the C-2,2' methine carbon bearing equatorial oxygen and is within ca. 1 ppm of that found for the corresponding carbon of the major conformation of **1** in solution at low temperature.<sup>6</sup> Its counterpart C-1,1' bearing an axial oxygen appears at 72.63 ppm, a result consistent with the well documented axial versus equatorial effects of oxygen on the directly bonded carbon of a cyclohexane ring.<sup>7</sup> The gauche- $\gamma$  effect of the axial oxygen will cause the resonance of C-5,5' to be shielded relative to that of C-4,4' which are trans- $\gamma$  to equatorial oxygen.<sup>7</sup> Hence the lines at 20.42 and 24.84 ppm respectively are assigned to these sites.

In the solid phase of **1**, C-3,3' and C-6,6' exhibit nearly identical chemical shifts at ca. 28 ppm, whereas for the major conformation in solution these resonances are at 28.02 and 26.61 ppm, respectively.

Distinction between C-7,7' and C-9,9' is made on the basis of the number of gauche type interactions in which each is involved in the crystal, either as a central or a terminal atom of a torsional

(7) Wilson, N. K.; Stothers, J. B. *Top. Stereochem.* 1973, 8, 1.

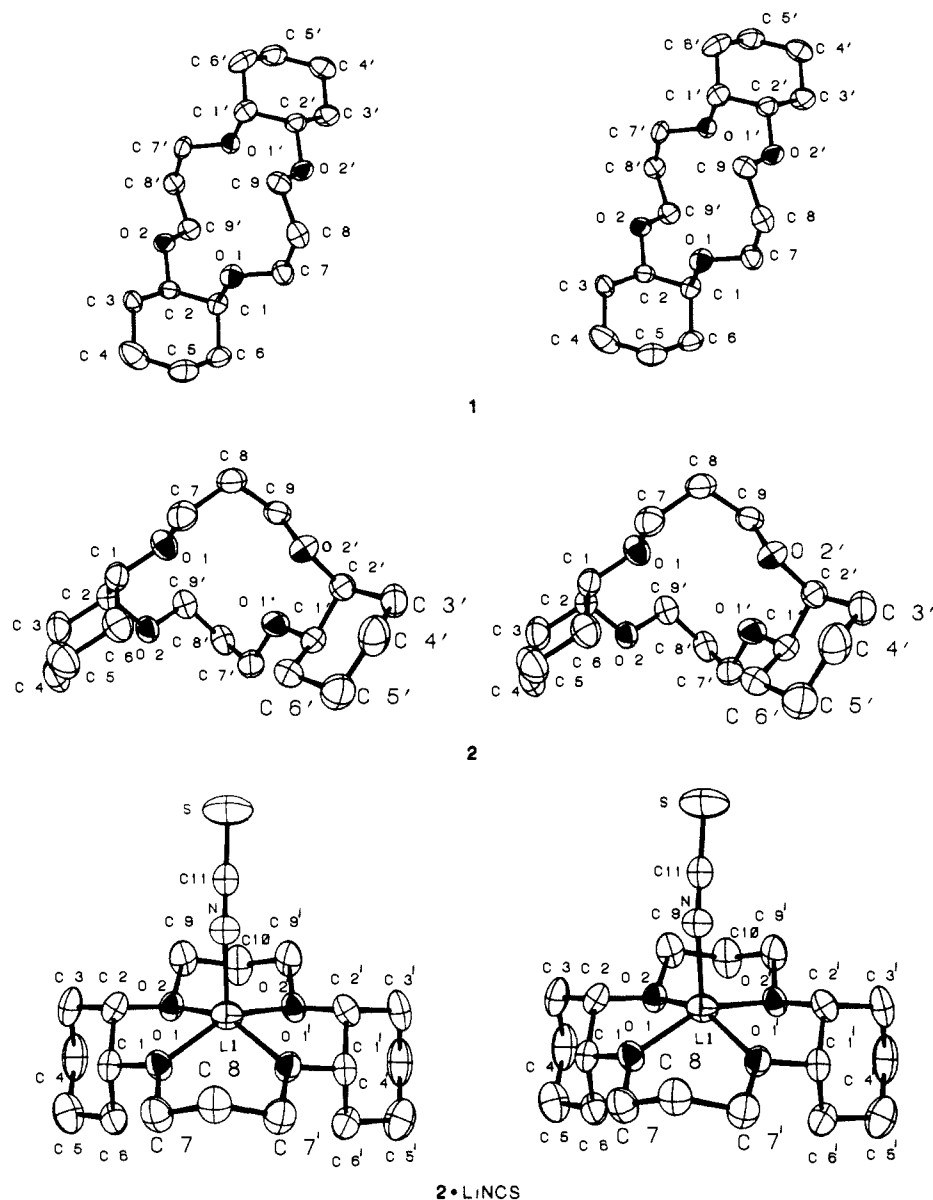
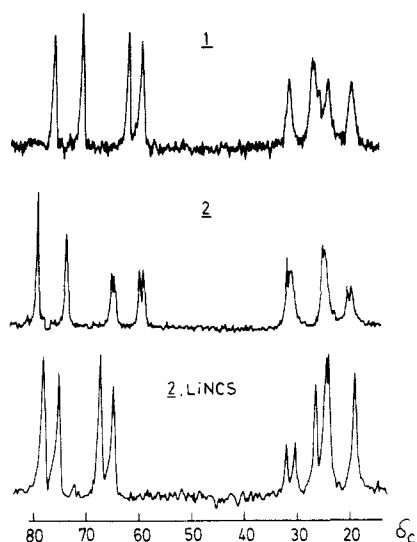
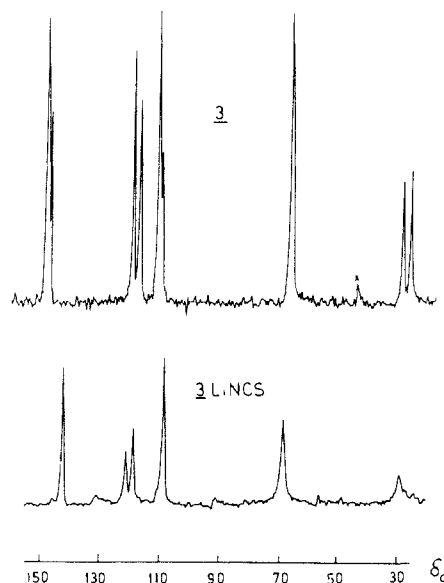


Figure 2. Stereoviews of 1, 2, and 2·LiNCS.

Figure 3. 45.3-MHz  $^{13}\text{C}$  CPMAS spectra of 1, 2, and 2·LiNCS.

network. C-9,9' is involved in three gauche-type interactions while C-7,7' has only two, with a third dihedral angle of  $81.7^\circ$ . The other two torsional interactions in each case (ignoring hydrogens)

Figure 4. 45.3-MHz  $^{13}\text{C}$  CPMAS spectra of 3 and 3·LiNCS.

are transoid in nature. On the basis of these considerations, we expect the resonance for C-9,9' to appear upfield from that for

Table II. Torsion Angles Involving Non-Hydrogen Atoms of 14-Crown-4 Ether Systems

14-crown-4						1				2		2-LiNCS			
atoms				value	atoms				value	value	atoms				value
O4	C7	C6	O3	77.1	O1	C1	C2	O2	56.9	64.2	O1	C1	C2	O2	55.4
C7	C6	O3	C5	-89.1	C9'	O2	C2	C1	65.1	-92.4	C1	C2	O2	C9	-178.7
C6	O3	C5	C4	167.8	C2	O2	C9'	C8'	170.4	175.6	C2	O2	C9	C1	-176.2
C3	C4	C5	O3	-70.6	C7'	C8'	C9'	O2	61.5	-62.6	O2	C9	C10	C9'	-71.4
O2	C3	C4	C5	-64.0	O1'	C7'	C8'	C9'	64.1	-58.5	C9	C10	C9'	O2'	71.4
C4	C3	O2	C2	179.0	C1'	O1'	C7'	C8'	-173.6	-174.8	C10	C9'	O2'	C2'	176.2
C3	O2	C2	C1	-172.0	C7'	O1'	C1'	C2'	157.9	174.0	C9'	O2'	C2'	C1'	178.7
O2	C2	C1	O1	75.9	O1'	C1'	C2'	O2'	-57.2	65.5	O2'	C2'	C1'	O1'	-55.3
C10	O1	C1	C2	-92.7	C9	O2'	C2'	C1'	-63.0	-91.6	C2'	C1'	O1'	C7'	-166.4
C9	C10	C1	O1	169.4	C2'	O2'	C9	C8	-169.9	172.1	C1'	O1'	C7'	C8	175.4
C8	C9	C10	O1	-69.3	C7	C8	C9	O2'	-65.5	-64.3	O1'	C7'	C8	C7	68.9
O4	C8	C9	C10	-64.7	O1	C7	C8	C9	-61.9	-58.8	C7'	C8	C7	O1	-68.9
C9	C8	O4	C7	176.9	C1	O1	C7	C8	172.9	-175.8	C8	C7	O1	C1	-175.4
C8	O4	C7	C6	-172.2	C7	O1	C1	C2	-158.2	177.3	C7	O1	C1	C2	166.4
					C1	C2	C3	C4	-54.7	-56.2	C1	C2	C3	C4	-56.1
					C2	C3	C4	C5	54.2	55.4	C2	C3	C4	C5	57.0
					C3	C4	C5	C6	-55.7	-54.4	C3	C4	C5	C6	-57.4
					C4	C5	C6	C1	57.6	55.1	C4	C5	C6	C1	56.6
					C2	C1	C6	C5	-56.5	-56.4	C2	C1	C6	C5	-56.8
					C6	C1	C2	C3	55.6	56.7	C6	C1	C2	C3	56.7
					C7	O1	C1	C6	82.0	-59.2	C7	O1	C1	C6	-71.4
					O1	C1	C6	C5	61.8	-177.6	O1	C1	C6	C5	-175.1
					O1	C1	C2	C3	-65.1	-177.7	O1	C1	C2	C3	178.3
					C9'	O2	C2	C3	-169.8	147.3	C9	O2	C2	C3	60.4
					O2	C2	C3	C4	179.1	64.7	O2	C2	C3	C4	62.2
					C6	C1	C2	O2	177.6	-61.5	C6	C1	C2	O2	-66.3
					C1'	C2'	C3'	C4'	54.6	-57.6	C1'	C2'	C3'	C4'	56.1
					C2'	C3'	C4'	C5'	-52.7	54.5	C2'	C3'	C4'	C5'	-57.0
					C3'	C4'	C5'	C6'	53.4	-52.6	C3'	C4'	C5'	C6'	57.4
					C4'	C5'	C6'	C1'	-54.3	54.0	C4'	C5'	C6'	C1'	-56.6
					C2'	C1'	C6'	C5'	55.4	-57.0	C2'	C1'	C6'	C5'	56.8
					C6'	C1'	C2'	C3'	-55.0	59.1	C6'	C1'	C2'	C3'	-56.7
					C7'	O1'	C1'	C6'	-81.5	-63.4	C9'	O2'	C2'	C3'	-60.4
					O1'	C1'	C6'	C5'	-64.1	-178.2	O2'	C2'	C3'	C4'	-62.2
					O1'	C1'	C2'	C3'	65.6	-175.7	C6'	C1'	C2'	O2'	66.3
					C9	O2'	C2'	C3'	172.0	148.0	C7'	O1'	C1'	C6'	71.4
					O2'	C2'	C3'	C4'	-179.4	63.6	O1'	C1'	C6'	C5'	175.1
					C6'	C1'	C2'	O2'	-177.7	-59.7	O1'	C1'	C2'	C3'	-178.3

Table III. Solid-Phase  $^{13}\text{C}$  Chemical Shifts ( $\delta_c$  from TMS  $\pm 0.1$ )

carbon	1	2	2-LiNCS	3	3-LiNCS
C-1	72.6	82.0	78.4	(148.0) <sup>a</sup>	146.0
C-1'		82.0			
C-2	78.0	76.3	75.8	(110.5) <sup>b</sup>	110.1
C-2'		76.3			
C-3	27.9	(32.0) <sup>a</sup>	27.0	(118.0) <sup>c</sup>	(120.8) <sup>a</sup>
C-3'		(32.0) <sup>a</sup>			
C-4	24.8	(19.8) <sup>b</sup>	19.1	(120.0) <sup>c</sup>	(123.2) <sup>a</sup>
C-4'		(20.9) <sup>b</sup>			
C-5	20.4	(25.2) <sup>c</sup>	(24.2) <sup>a</sup>	(111.8) <sup>b</sup>	110.1
C-5'		(25.2) <sup>c</sup>			
C-6	27.9	(25.7) <sup>c</sup>	(24.9) <sup>a</sup>	(149.3) <sup>a</sup>	
C-6'		(25.7) <sup>c</sup>			
C-7	63.5	(60.9) <sup>d</sup>	(65.2) <sup>b</sup>	67.0	68.2
C-7'		(61.8) <sup>d</sup>			
C-8	32.6	(32.9) <sup>a</sup>	30.7	(26.6) <sup>d</sup>	27.3
C-8'		(32.9) <sup>a</sup>			
C-9	60.8	(67.3) <sup>e</sup>	(67.6) <sup>b</sup>	67.0	68.2
C-9'		(66.6) <sup>e</sup>			
C-10			32.6	(29.3) <sup>d</sup>	27.3

<sup>a-e</sup> Indicate possible interchange of resonance assignments.

the C-7,7' position. In this instance the chemical shift difference is 2.70 ppm.

The remaining line in the spectrum of **1** at 32.61 ppm is attributed to the C-8,8' site and its shift is within ca. 2 ppm of that found for the corresponding carbon of the major conformer of **1** in solution at 193 K.<sup>6</sup> The observation of a single resonance for these positions is consistent with the presence of a center of

symmetry in **1** as opposed to a plane passing through C-8,8'.

(ii) *cis-syn-cis*-Dicyclohexano-14-crown-4 (**2**). The X-ray crystallographic data for this material indicate that the molecule possesses molecular pseudosymmetry in the form of a local twofold rotational axis with the following direction cosines: (-0.75 (5), -0.34 (5), 0.56 (6)). In order to assess the deviation to twofold symmetry from the positions of the atoms and their twofold related counterparts, the molecule was positioned in an orthogonal reference system with its pseudolocal twofold axis aligned along the z axis. The following averaged fractional differences were obtained: 0.031, 0.004, and 0.002. These numbers are respectively 208, 21, and 19 times the standard deviations in the atomic coordinates, showing clearly that **2** does not have true twofold symmetry.

It is of interest to compare the conformations of the 14-membered rings of **1** and **2** with that found for 14-crown-4 itself.<sup>1</sup> For **2** the macrocycle and 14-crown-4 have approximately the same conformation, with torsion angles differing by 1-8°. Most of the torsion angles involving the C-C bond shared between the cyclohexyl and the 14-membered rings show larger differences which average ca. 12°. The presence of cyclohexyl substituents on the 14-crown-4 renders **2** less flexible at the substituted carbons than is the case for 14-crown-4 itself. Also the O-C-C-O torsion angles in **2** are held closer to the ideal value of 60° for a true gauche interaction because of the *cis* deposition of the cyclohexyl substituents.

In contrast to these results are the X-ray data for **1**. Large differences in the absolute values of the torsional angles (27-29°) in the C9'-O2-C2-C1 and C9-O2'-C2'-C1' angles of **1** compared

Table IV. Crystallographic Data

	1	2	2-LiNCS
formula	C <sub>18</sub> H <sub>32</sub> O <sub>4</sub>	C <sub>18</sub> H <sub>32</sub> O <sub>4</sub>	C <sub>19</sub> H <sub>32</sub> O <sub>4</sub> SNLi
fw	312.34	312.34	377.70
isomer	cis-anti-cis	cis-syn-cis	cis-syn-cis
cryst system	orthorhombic	monoclinic	orthorhombic
space group	<i>Pbc</i> 21	<i>P</i> 21/ <i>a</i>	<i>Pn</i> ma
<i>a</i> , Å	8.25994 (16)	14.2078 (17)	9.7300 (3)
<i>b</i> , Å	10.13769 (20)	8.5183 (8)	12.0069 (4)
<i>c</i> , Å	20.7873 (4)	15.0961 (19)	17.7338 (5)
β, deg		102.920 (10)	
<i>V</i> , deg	1740.66	1780.77	2071.79
<i>Z</i> (molecules/cell)	4	4	4
<i>D<sub>c</sub></i> , g cm <sup>-3</sup>	1.192	1.165	1.210
cryst dims, mm <sup>3</sup>	0.20 × 0.40 × 0.40	0.30 × 0.35 × 0.40	0.02 × 0.40 × 0.40
radiation (λ, Å)	Cu Kα <sub>1</sub> (1.54056 Å)	Mo Kα <sub>1</sub> (0.70932 Å)	Cu Kα <sub>1</sub> (1.54056 Å)
octants measd	<i>hkl</i> , <i>-hkl</i>	<i>hkl</i> , <i>-hkl</i>	<i>hkl</i> , <i>-h</i> , <i>-k</i> , <i>-l</i>
max 2θ	151.9	45.0	129.5
no. of unique reflns	1980	2337	1831
no. of obsvd reflns	1752	1767	1312
( <i>I</i> / <i>σ</i> ( <i>I</i> ) ratio)	2.5	2.5	2.5
av std fluctuatns, %	0.47	0.39	0.61
abs coeff, mm <sup>-1</sup>	0.62	0.07	1.52
<i>R</i>	0.053	0.030	0.058
<i>R<sub>w</sub></i>	0.038	0.018	0.037
<i>S</i> (GOF)	4.453	2.628	4.025

to the corresponding torsion angle values for **2** indicate clearly the very different conformations of the aliphatic -O-(CH<sub>2</sub>)<sub>3</sub>-O- side chains present in **1** and **2**.

In all other respects, the bond angles for **1**, **2**, and 2-LiNCS are in good agreement with the published data for 14-crown-4 itself<sup>1</sup> as are the C-C and C-O bond distances.

The lack of any "true" symmetry elements in **2** is readily apparent in the <sup>13</sup>C CPMAS spectrum (Figure 3). For example, four resonances are obtained for CH<sub>2</sub> carbons bearing oxygen in the range of 61–68 ppm. This indicates clearly that the C-7,9,7', and 9' sites are nonequivalent in contrast to the situation for **1** where only two resonances were found for the corresponding carbons.

For **2**, the chemical shift difference between cyclohexyl carbons bearing axial versus equatorial oxygen is approximately the same as that in **1**, although each of these carbons in **2** is deshielded by ca. 4 ppm relative to the corresponding center in **1**. The carbon bearing equatorial oxygen is again deshielded relative to its counterpart with an axial oxygen.<sup>7</sup> From the spectrum of **2** it is evident that the minor differences in the environments of C-1 and C-1' are not sufficient to cause resolvable <sup>13</sup>C chemical shifts for these sites. Similarly C-2 and C-2' have coincident <sup>13</sup>C resonance positions in the solid.

In the case of the CH<sub>2</sub> oxygenated carbons of **2** the observed resonances occur as two pairs of doublets. Although **2** possesses no true symmetry elements, the environments of C-7 and C-7' are clearly very similar from the X-ray data as the environments of C-9 and C-9'. Hence the chemical shifts expected for these "pseudoequivalent" pairs are expected to be nearly identical. It is interesting to compare the torsion angles of C-7,7' and C-9,9' of **2** with those for C-7,7' and C-9,9' of **1**. It is evident from Table II that C-9,9' of **1**, which appears in the <sup>13</sup>C spectrum at 60.76 ppm, has very similar torsion angles to the C-7 and C-7' sites of **2**. Therefore one can confidently assign the <sup>13</sup>C shift at 60.98 and 61.84 ppm of **2** to these carbons. The C-9,9' carbons of **2** are thus deshielded by ca. 6 ppm relative to C-7,7'.

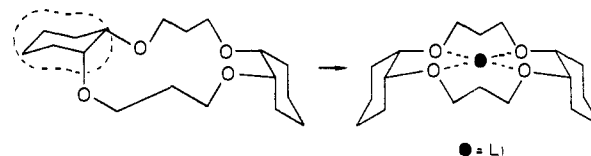
The C-9,9' carbons of **2** have two unique torsional geometries relative to C-7,7'. Specifically these are the C9-O2'-C2'-C3' network with a torsion angle of ca. 148° and the C9-O2'-C2'-C1' network having an angle of ca. 92°. The angles for the corresponding networks involving C-7,7' are ca. 175 and 61°, respectively. Detailed calculations regarding the dihedral angle dependence of <sup>13</sup>C chemical shifts for these types of networks are not yet available. On the basis of the results of INDO MO <sup>13</sup>C chemical shift calculations for butane,<sup>8</sup> it is likely, however, that

the major factor in the observed deshielding of C-9,9' is the change in the torsion angle for the C9-O2'-C2'-C1' network to nearly a perpendicular geometry (92°) from a nearly pure gauche type geometry (61°).

The nonoxygenated carbons, C-4 and C-4' which are gauche-γ to an axial oxygen, appear at the highest field position, near 20 ppm. Their counterparts C-5 and C-5' which are trans-γ to equatorial oxygen appear as a double intensity pair of lines near 25 ppm. For the macrocyclic carbons C-8 and C-8' a double intensity resonance near 32 ppm is observed. Assignments of resonances for C-3,3' versus C-6,6' were made by consideration of the known stereochemical dependence of cyclohexyl carbon shifts on the axial versus equatorial orientation of OCH<sub>3</sub> substituents.<sup>9</sup>

Finally it is of interest to note that the chemical shifts of solid **2** are within 1.5 ppm of those found for the corresponding carbons of this molecule in solution under conditions where ring inversion is slow on the NMR time scale.<sup>10</sup> In contrast to the situation for **1**, **2** undergoes only one degenerate conformational process which can be detected by NMR. This appears to be a double cyclohexane ring inversion which is accompanied by a reorganization of the 14-membered ring geometry.

(iii) LiNCS Complex of **2**. The X-ray crystal structure of this complex (Figure 2) shows that it possesses a crystallographic mirror plane of symmetry passing through C-8 and C-10. Comparison of the X-ray structures of free **2** and its LiNCS complex indicates that inversion of one of the cyclohexane rings has occurred in the complex as depicted below. Thus the symmetry of **2** changes from local pseudo-2-fold to crystallographic mirror symmetry upon Li complexation.



This produces a geometry in which the four oxygen atoms are positioning themselves in order to bind to Li as efficiently as possible. Such a geometry was not present in free **2** and hence a type of "molecular recognition" has occurred in order to form this complex.

The diagonal distance across the ring between opposite oxygens is 3.88 Å. Taking into account the van der Waals radius of oxygen,

(9) Schneider, H.-J.; Hoppen, V. *Tetrahedron Lett.* 1974, 579.

(10) Buchanan, G. W.; Kirby, R. A.; Morat, C. *Can. J. Chem.*, submitted for publication.

(8) Seidman, K.; Maciel, G. E. *J. Am. Chem. Soc.* 1977, 99, 659.

1.4 Å, the resulting adjusted diameter of the cavity is 1.08 Å which is slightly too small to fit the Li cation (effective diameter 1.18–1.52 Å)<sup>11</sup> within the plane of the oxygens. The four oxygens are coplanar and Li cation is 0.55 Å out of this plane. In the X-ray structure of 3-LiNCS,<sup>2</sup> the adjusted diameter of the cavity was 0.97 Å, with Li<sup>+</sup> lying 0.79 Å above the plane of the four ethereal oxygen atoms. These structural features are consistent with expectations since dibenzo-14-crown-4 with its two aromatic rings is expected to be more rigid than its dicyclohexyl analogue **2** and thus exhibit a smaller effective cavity size.

The lithium atom is coordinated by the four oxygens and the nitrogen of the SCN anion in a distorted square-pyramidal geometry. The two Li–O(1) distances of 1.958 (6) Å are rather short and correspond more to the Li–O bond lengths in tetrahedral complexes (mean value 1.98 Å). The Li–O2 distances of 2.074 (6) Å seem to be normal for lithium–ethereal oxygen bond distances in pentacoordinated complexes with macrocyclic ligands.<sup>12</sup> Since the Li–O2 distances are longer, this implies that the Li cation does not lie exactly above the gravity center of the four oxygens. This is also demonstrated by the unsymmetrical nature of the O–Li–NCS bond angle values, with O(1)–Li–N angles larger than O(2)–Li–N angles.

The <sup>13</sup>C CPDAS spectrum of **2**-LiNCS shows ten clearly resolved resonances with relative intensities that reflect the mirror plane of symmetry that is present. The carbon bearing equatorial oxygen, C-1, is again deshielded relative to its counterpart C-2 with an axial substituent, but in this case the chemical shift difference of 2.59 ppm is only ca. 50% of that found for the corresponding carbons of **1** and **2**. The resonance at 19.1 ppm is assigned to C-4 which is gauche-γ to the axial oxygen O-2, while its counterpart C-5 which is trans-γ to O-1 is deshielded by ca. 5 ppm.

Distinction between resonances for C-8 and C-10 was made on the basis of their torsional environments in the X-ray structure. These environments are essentially identical (i.e., within 3°) except for one network. For C-8 there is a torsional network C8–C7–O1–Li in which the torsion angle is 21.47°, while the corresponding C-10 network C10–C9–O2–Li has a dihedral angle of 65.58°. In light of the previous discussion regarding the angular dependence of γ-shifts in <sup>13</sup>C NMR, we attribute the line at 30.7 to C-8 and that at 32.6 to C-10. Distinction between C-7 and C-9 was not deemed to be realistically possible. Each of these carbons is involved in nine torsional networks, and the 2.4 ppm chemical shift difference found between them is probably the result of the contribution of several factors.

(iv) **Dibenzo-14-crown-4 (3)**. No X-ray structure for this material is presently available. The <sup>13</sup>C spectrum in solution exhibits five resonances at δ<sub>c</sub> = 29.33, 67.32, 115.64, 121.75, and 149.48. The solid-phase <sup>13</sup>C CPDAS spectrum (Figure 4) shows nine resolved lines. If **3** possessed a center of symmetry in the crystal, then nine lines would be expected in the solid-phase <sup>13</sup>C spectrum; however, only a single resonance would be observed for the C-8 sites. In fact two absorptions are observed for these carbons in the range of 26–30 ppm, indicating that the crystal cannot possess a center of symmetry. The most likely situation is that there is a twofold axis or a plane of symmetry present in solid **3**. On this basis one would expect to observe ten resonances in the <sup>13</sup>C CPDAS spectrum. It appears that there is one case of accidental peak overlap at 67 ppm for the CH<sub>2</sub> carbons bearing oxygen, and hence the asymmetric unit in the crystal of **3** is one-half the molecule.

Of course in the absence of X-ray data one cannot rule out crystal packing phenomena or the existence of two different molecules in the crystal as the cause of the spectral multiplicity,<sup>3</sup> but the occurrence of such phenomena is relatively rare.

(v) **LiNCS Complex of 3**. The X-ray structure of this complex has been published<sup>2</sup> and there is a mirror plane of symmetry which bisects C-8, C-10, Li, and the SCN<sup>-</sup> part of the molecule. On

Table V. Atomic Parameters *x*, *y*, *z* and *B*<sub>iso</sub><sup>a</sup> (Esd's Refer to the Last Digit Printed)

	<i>x</i>	<i>y</i>	<i>z</i>	<i>B</i> <sub>iso</sub>
<b>1</b>				
O1	0.7029 (5)	0.1091 (3)	0.80879	3.45 (16)
O2	0.4960 (4)	0.2268 (3)	0.8986 (3)	3.25 (16)
O1'	0.7971 (4)	0.1610 (3)	1.01572 (17)	2.96 (13)
O2'	1.0091 (4)	0.0415 (3)	0.9250 (3)	3.20 (17)
C1	0.6390 (6)	0.2346 (4)	0.7954 (3)	2.71 (18)
C2	0.4820 (6)	0.2464 (6)	0.8316 (4)	2.92 (20)
C3	0.3555 (6)	0.1509 (5)	0.8080 (3)	2.98 (21)
C4	0.3269 (9)	0.1643 (8)	0.7345 (4)	5.4 (3)
C5	0.4823 (9)	0.1515 (7)	0.6981 (5)	4.4 (3)
C6	0.6075 (7)	0.2520 (6)	0.7221 (3)	3.80 (23)
C7	0.8745 (6)	0.1039 (5)	0.7978 (4)	3.58 (23)
C8	0.9369 (6)	-0.0296 (5)	0.8216 (3)	3.21 (21)
C9	0.9120 (6)	-0.0516 (5)	0.8932 (3)	3.22 (20)
C1'	0.8640 (7)	0.0333 (5)	1.0287 (3)	3.26 (22)
C2'	1.0228 (6)	0.0214 (5)	0.9932 (4)	2.90 (21)
C3'	1.1510 (9)	0.1179 (6)	1.0189 (3)	3.7 (3)
C4'	1.1739 (8)	0.1023 (6)	1.0898 (3)	4.2 (3)
C5'	1.0132 (9)	0.1106 (6)	1.1268 (5)	4.4 (3)
C6'	0.8906 (9)	0.0161 (6)	1.1010 (3)	4.5 (3)
C7'	0.6266 (6)	0.1679 (5)	1.0254 (3)	3.32 (21)
C8'	0.5687 (7)	0.3017 (6)	1.0031 (3)	3.50 (22)
C9'	0.5914 (7)	0.3252 (5)	0.9316 (3)	3.50 (21)
<b>2</b>				
O1	0.43178 (8)	0.10605 (14)	0.71276 (7)	3.94 (6)
O2	0.30918 (8)	0.35471 (14)	0.63137 (8)	3.88 (6)
O1'	0.45496 (8)	0.47611 (13)	0.83364 (8)	3.98 (6)
O2'	0.60305 (8)	0.25021 (14)	0.89997 (7)	3.44 (6)
C1	0.40994 (15)	0.12920 (25)	0.61668 (13)	3.86 (11)
C2	0.30985 (15)	0.20295 (24)	0.59145 (12)	3.76 (11)
C3	0.27913 (19)	0.2255 (3)	0.48925 (15)	5.18 (14)
C4	0.35122 (20)	0.3221 (3)	0.45325 (16)	5.51 (16)
C5	0.45159 (21)	0.2517 (4)	0.47953 (16)	5.83 (15)
C6	0.48289 (17)	0.2274 (3)	0.58212 (15)	4.63 (13)
C7	0.52071 (16)	0.0317 (3)	0.75020 (14)	4.09 (12)
C8	0.52780 (16)	0.00652 (24)	0.85035 (4)	3.89 (11)
C9	0.52175 (14)	0.15438 (24)	0.90310 (13)	3.46 (10)
C1'	0.55331 (14)	0.52102 (22)	0.86445 (12)	3.47 (11)
C2'	0.60000 (13)	0.40380 (23)	0.93722 (12)	3.23 (10)
C3'	0.70333 (15)	0.4522 (3)	0.97826 (14)	4.07 (11)
C4'	0.76206 (16)	0.4648 (3)	0.90586 (16)	4.85 (13)
C5'	0.71459 (17)	0.5735 (3)	0.82959 (17)	5.17 (13)
C6'	0.60949 (15)	0.5298 (3)	0.79018 (14)	4.15 (11)
C7'	0.39519 (17)	0.5797 (3)	0.77133 (16)	4.55 (13)
C8'	0.29342 (15)	0.5185 (3)	0.75455 (14)	4.31 (12)
C9'	0.28380 (14)	0.3546 (3)	0.71743 (13)	3.86 (12)
<b>2-LiNCS</b>				
S	0.37282 (18)	1/4	0.44365 (9)	7.13 (11)
O1	-0.20400 (2)	0.36679 (17)	0.49047 (11)	3.21 (10)
O2	-0.09315 (25)	0.37099 (18)	0.35501 (11)	3.30 (11)
N	0.0951 (5)	1/4	0.4780 (3)	4.4 (3)
C1	-0.2170 (4)	0.4692 (3)	0.44785 (18)	3.09 (16)
C2	-0.0924 (4)	0.4740 (3)	0.39740 (18)	3.39 (18)
C3	-0.0981 (6)	0.5783 (3)	0.34764 (22)	4.56 (23)
C4	-0.2311 (6)	0.5814 (3)	0.0205 (23)	5.6 (3)
C5	-0.3547 (6)	0.5767 (4)	0.35375 (25)	5.20 (24)
C6	-0.3505 (4)	0.4719 (3)	0.40330 (21)	3.79 (19)
C7	-0.2928 (5)	0.3564 (3)	0.55338 (20)	3.89 (19)
C8	-0.2579 (7)	1/4	0.5949 (3)	3.7 (3)
C9	0.0197 (5)	0.3578 (3)	0.30428 (22)	4.58 (22)
C10	-0.0003 (8)	1/4	0.2601 (3)	5.2 (3)
C11	0.2101 (6)	1/4	0.4645 (3)	3.5 (3)
LI	-0.1005 (9)	1/4	0.4384 (4)	3.5 (4)

<sup>a</sup> *B*<sub>iso</sub> is the mean of the principal axes of the thermal ellipsoid.

this basis one expects to observe ten unique <sup>13</sup>C resonances in the solid for this complex. This assumes that no thiocyanate resonances would be observed due to quadrupolar broadening. Experimentally one sees from aromatic and two aliphatic carbon resonances for this complex, there being two instances of accidental peak overlap in the aromatic region and two in the aliphatic portion of the spectrum. The chemical shifts in the complex are within 1 ppm of those for **3**, except for the aromatic carbons bearing

(11) Shannon, R. D. *Acta Crystallogr.* **1976**, *A32*, 751.

(12) Shoham, G.; Lipscomb, W. N.; Olsher, U. *J. Am. Chem. Soc.* **1983**, *105*, 1247.

oxygen which are shielded by 2.0–3.3 ppm relative to free 3.

### Experimental Section

(a) **Spectra.** The  $^{13}\text{C}$  CPMAS spectra were recorded at 45.3 MHz on a Bruker CXP-180 spectrometer. Cross polarization times were typically 3 ms, with the radio frequency field amplitude being 60 kHz. Satisfactory signal-to-noise ratios were obtained after a maximum of 400 spectral accumulations. The sweep width was 20 kHz with a recycle time of 4–8 s. Normally 2K data points were collected with zero filling to 8K before Fourier transformation. Magic-angle spinning rates of ca. 3 kHz were obtained with use of Kel-F spinners of the Andrew-Beams type. Chemical shifts were measured relative to external solid hexamethylbenzene (HMB) and converted to the TMS scale via the factor of 16.9 ppm, which is the chemical shift for the  $\text{CH}_3$  group of HMB.

(b) **Crystallographic Measurements and Structure Solutions.** Single crystals of **1** and **2**-LiNCS were mounted on a Nonius CAD4 diffractometer controlled by the NRCCAD software<sup>13</sup> while an automated Picker 4-circle diffractometer was used for the single crystal of **2**. Accurate cell parameters and intensity data were obtained at room temperature with use of graphite-monochromatised Cu K radiation for **1** and **2**-LiNCS and graphite-monochromatised Mo K radiation for **2**.

The data were corrected for the Lorentz effect and measured direct beam polarization<sup>14</sup> but not for absorption. The cell parameters were obtained by least-squares refinement of the setting angles of 89 ( $90^\circ < 2\theta < 98^\circ$ ) for **1**, 42 ( $90^\circ < 2\theta < 98^\circ$ ) for **2**-LiNCS, and 60 reflections ( $35^\circ < 2\theta < 45^\circ$ ) for **2**. Other specific details are provided in Table IV.

The intensity data for **1** and **2**-LiNCS revealed systematic absences consistent with two possible space groups in each case. These are *Pbc2<sub>1</sub>* and *Pbcm* for **1** and *Pnma* and *Pn2<sub>1</sub>a* for **2**-LiNCS. The space group *P2<sub>1</sub>/a* was uniquely defined from the systematic absences noted in the data set of **2**. The structure of **1** was solved assuming at first the acentric space group *Pbc2<sub>1</sub>*. The structure of **2** was solved in space group *Pnma*.

The positions of the non-hydrogen atoms in the three structures were determined by direct methods with MULTAN.<sup>15</sup> At this stage isotropic refinement of all non-hydrogen atoms was carried out by full-matrix least-squares. All hydrogen atoms of **1**, **2**, and **2**-LiNCS were then located on a difference map. They were included and refined isotropically while non-hydrogen atoms were refined anisotropically. Full-matrix least-squares refinements were carried out with weights based on counting statistics ( $1/\sigma(F_0)^2$ ). The final difference Fourier maps were featureless with general background lower than  $\pm 0.24$ , 0.13, and 0.38  $e/\text{\AA}^3$ , for **1**, **2**, and **2**-LiNCS, respectively. All computations were performed with the NRCVAX system of programs.<sup>16</sup>

As the space group of **1** could be *Pbcm*, cell symmetry was checked with the program MISSYM which finds all metric symmetry elements from the atomic coordinates of any crystal structure and builds the generators in the unit cell.<sup>17</sup> Only symmetry elements of the first assumed space group, *Pbc2<sub>1</sub>*, could be found. Furthermore the packing diagram of **1**

(Figure 5, Supplementary Material) does not show mirror symmetry parallel to the *ab* plane of the unit cell.

The scattering curves were from standard sources.<sup>18</sup> The refined coordinates of non-hydrogen atoms for all compounds are listed in Table V.

(c) **Materials.** Dibenzo-14-crown-4 (**3**) was prepared according to the published procedure<sup>19</sup> with the exception of the hydrolysis of 1,3-bis(*o*-methoxyphenoxy)propane to 1,3-bis(*o*-hydroxyphenoxy)propane. This was accomplished selectively via the trimethylsilyl iodide reagent.<sup>20</sup> A typical procedure follows. A mixture of 8.0 g (0.28 mol) of 1,3-bis(*o*-methoxyphenoxy)propane and 9.07 mL (0.067 mol) of trimethylsilyl iodide was dissolved in 200 mL of methylene chloride and refluxed with stirring for 20 h. With continued stirring and discontinued heating 100 mL of distilled water was added. After 1 h the organic phase was separated and dried and the solvent was evaporated to yield 6.5 g of crude crystals. Recrystallization from methylene chloride and hexanes yielded 4.07 g (56% yield) of white needles, mp 147–149 °C (lit.<sup>19</sup> mp 150–151 °C).

Hydrogenation of **3** to a mixture of **1** and **2** was accomplished with use of an American Instrument Co. 50 000 psi maximum pressure high pressure apparatus. In 60 mL of 1-butanol was dissolved 1.2 g (.004 mol) of **3** and 0.75 g of 5% ruthenium on aluminum catalyst. A pressure of  $\text{H}_2$  gas of 1500 psi was used and the reaction was continued for 6 h at a temperature of 110 °C. The catalyst was removed by filtration and the butanol by rotary evaporation at 70 °C. Recrystallization from methylene chloride and hexanes yielded **1**, mp 149–151 °C. Column chromatography of the mother liquors was carried out on silica gel with a 20:1 methylene chloride: diethyl ether solvent mixture. Initial fractions contained a mixture of **1** and **2**, while the latter fractions had only **2** present. Recrystallization of these latter column fractions from hexanes yielded pure **2**, mp 96–98 °C.

The LiNCS complex of **2** was prepared according to the following procedure. Equimolar amounts of **2** and LiNCS were dissolved in a minimum quantity of dry methanol and allowed to stand for 2–3 h. The solvent was removed by rotoevaporation and the resulting solid was recrystallized from a mixture of methylene chloride and hexanes containing a trace of methanol. The sample of **2**-LiNCS which was employed for X-ray analysis had a melting point of 208–209 °C. A similar method was employed for the synthesis of **3**-LiNCS<sup>2</sup> which exhibited a melting point above 300 °C.

**Acknowledgment.** G.W.B. thanks Dr. J. A. Ripmeester for his hospitality and provision of facilities for obtaining the  $^{13}\text{C}$  CPMAS spectra. Financial support from NSERC is acknowledged.

**Registry No.** **1**, 112457-82-6; **2**, 113473-91-9; **2**-LiNCS, 113430-82-3; **3**, 14174-06-2; **3**-LiNCS, 113430-83-4.

**Supplementary Material Available:** Table 6 listing anisotropic temperature factors, Table 7 listing thermal and atomic parameters of hydrogen atoms, and Figure 5 containing the packing diagram of **1** (6 pages); Table 8 containing observed, unobserved, and calculated structure factor amplitudes (43 pages). Ordering information is given on any current masthead page.

(13) LePage, Y.; White, P. S.; Gabe, E. J. *ACA Meeting Abstr.* **1986**, *14*, 24.

(14) LePage, Y.; Gabe, E. J.; Calvert, L. D. *J. Appl. Crystallogr.* **1979**, *12*, 25.

(15) Germain, G.; Main, P.; Woolfson, M. M. *Acta Crystallogr.* **1971**, *A27*, 368.

(16) Gabe, E. J.; Lee, F. L.; LePage, Y. In *Crystallographic Computing 3*; Sheldrick, C., Krueger, C., Goddard, R., Eds.; Clarendon Press: Oxford, 1985; p 167.

(17) LePage, Y. *ACA Meeting Abstr.* **1986**, *14*, 17.

(18) *International Tables for X-ray Crystallography*, 2nd ed.; Kynoch Press: Birmingham, 1974; Vol. 4.

(19) Pedersen, C. J. *J. Am. Chem. Soc.* **1967**, *89*, 7017.

(20) Jung, M. E.; Lyster, M. A. *J. Org. Chem.* **1977**, *42*, 3761.